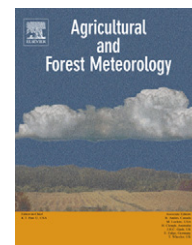


available at [www.sciencedirect.com](http://www.sciencedirect.com)journal homepage: [www.elsevier.com/locate/agrformet](http://www.elsevier.com/locate/agrformet)

## Evaluating climatic and soil water controls on evapotranspiration at two Amazonian rainforest sites

Rosie A. Fisher<sup>a,\*</sup>, Mathew Williams<sup>a</sup>, Maria de Lourdes Ruivo<sup>b</sup>,  
Antonio Lola de Costa<sup>c</sup>, Patrick Meir<sup>a</sup>

<sup>a</sup>School of GeoSciences, University of Edinburgh, Edinburgh, UK

<sup>b</sup>Museu Paraense Emilio Goeldi, Belém, Pará, Brazil

<sup>c</sup>Universidade Federal do Pará, Belém, Pará, Brazil

### ARTICLE INFO

#### Article history:

Received 25 July 2007

Received in revised form

28 November 2007

Accepted 3 December 2007

#### Keywords:

Amazon

Soil moisture

Hydraulic conductivity

Gas exchange

### ABSTRACT

Interactions between the biosphere and the atmosphere have profound impacts on the functioning of the Earth system. One of the most important areas of biosphere–atmosphere interaction is the Amazon basin, which plays a key role in the global cycles of carbon, water and energy. The Amazon is vulnerable to climatic change, with increasingly hot and dry conditions expected over the next 50–100 years in some models. The resulting loss of carbon from the Amazon basin has been suggested as a potentially large positive feedback in the climate system. We investigated the differences in atmospheric demand and soil water availability between two sites; Manaus, in central Amazonia, where evapotranspiration was limited in the dry season, and Caxiuanã in eastern Amazonia, where it was not. New soil hydraulic data including water release and unsaturated hydraulic conductivity curves were collected at Caxiuanã using the instantaneous profile method (IPM), pressure plate analysis and tension infiltrometry. These data were compared to existing data from Manaus. The plant available soil water at the Caxiuanã site was 2.1–3.4 times larger than the Manaus site. The hydraulic conductivity curves indicated the existence of a secondary macropore structure at very low tensions (–0.05 kPa to –1 kPa), potentially caused by biogenic macropores, but did not vary with respect to soil water potential between sites. In addition, differences in the climatic severity of the dry season were estimated. The maximum soil water deficit, projected using a simple model of forest water use, was similar between the sites. No difference in climatic severity between sites was found and we conclude that below-ground supply of water, rather than climatic differences, were likely to have caused the contrasting dry season behaviour at the two sites. These findings indicate that, in combination with other factors, heterogeneity in soil water retention capacity may exert strong controls on the spatial variation in forest responses to climatic change.

© 2007 Elsevier B.V. All rights reserved.

## 1. Introduction

Recent analyses using coupled climate and carbon cycle models indicate that during the next 100 years, the net

feedback between the biosphere and atmosphere is likely to be positive, and to add between 20 and 200 ppm to atmospheric CO<sub>2</sub> concentrations by 2100 (Friedlingstein et al., 2006; Salazar et al., 2007). The majority of model simulations predicted a

\* Corresponding author. Present address: Department of Animal and Plant Sciences, University of Sheffield, Sheffield, UK.  
Tel.: +44 114 222 4649.

E-mail address: [rosie.fisher@sheffield.ac.uk](mailto:rosie.fisher@sheffield.ac.uk) (R.A. Fisher).  
0168-1923/\$ – see front matter © 2007 Elsevier B.V. All rights reserved.  
doi:10.1016/j.agrformet.2007.12.001

major decline in land carbon storage, located in tropical forests and the Amazon basin in particular, which leads to an increased accumulation of carbon dioxide in the atmosphere. The recently published fourth IPCC assessment report (Figure SPM7. IPCC, 2007) suggests that, over large areas of Southern and Eastern Amazonia, more than 90% of GCM model predictions agree that dry season rainfall will decline by 10–30%. In Northern and Central areas, there is no agreement between GCMs and in Western Amazonia, a slight increase in precipitation rates is predicted. In addition, increases in temperature are uniformly predicted to rise across the whole region. Understanding the interaction between the drying climate and forest carbon dioxide exchange in Amazonia is therefore of fundamental importance to the prediction of future biosphere–atmosphere feedback in the climate system (Huntingford et al., 2004; Werth and Avissar, 2004).

At present, many of the forests of Southern and Eastern Amazonia experience, on average, a dry season exceeding three months, where rainfall is less than  $3 \text{ mm day}^{-1}$  (Sombroek, 2001). High temperatures and radiation create an evaporative demand in the Amazonian region that is typically  $3\text{--}4 \text{ mm day}^{-1}$  (Malhi et al., 2002; Werth and Avissar, 2004; Cox et al., 2004; Huntingford et al., 2004). This means that, during the dry season, plants must utilize water stored in soils to supply evapotranspiration at a rate which is unlimited by water availability (Nepstad et al., 1994; Hodnett et al., 1996). Despite this long dry season, it is not yet clear to what extent the evapotranspiration of contemporary Amazonian rainforests is limited by water availability. Most ecosystem models of Amazonian evapotranspiration predict very large reductions in water use during the dry season (Tian et al., 1998; Potter et al., 2001; Werth and Avissar, 2004). In contrast to these model expectations, recent Earth observation data have suggested that Amazonian ecosystems can be observed to ‘green-up’ during the dry season (Huete et al., 2006) and even during the recent 2005 El Niño event (Saleska et al., 2007). However, it is not clear whether these data represent changes in leaf area or in the observed chlorophyll content of the visible leaves, and how they might relate to changes in photosynthetic rates. Furthermore, existing evidence of forest evapotranspiration from micrometeorological eddy covariance measurements at six locations show contrasting results. At five locations, no evidence of hydraulic limitation of evapotranspiration has been measured (Grace et al., 1996; Araújo et al., 2002; Carswell et al., 2002; Saleska et al., 2003; da Rocha et al., 2004; Goulden et al., 2004). At one site, Manaus, in central Amazonia, the observed evapotranspiration declined by up to 50% in response to low soil moisture during the 1995–96 dry season (Williams et al., 1998; Malhi et al., 1998, 2002). Because these data are the only data where a reduction in gas exchange in the dry season has been observed, they have been used for calibration of global models of gas exchange (Harris et al., 2004) and used to make predictions concerning the rate of Amazon die-back (Huntingford et al., 2004). However, the cause of the different responses to rainfall seasonality between sites is unknown, and therefore the likely spatial and temporal extent of these different modes of behaviour cannot be estimated.

In this paper, we investigated two possible explanations for the differences in dry season evapotranspiration between the

Manaus site and a site at Caxiuanã, in Eastern Amazonia. The Caxiuanã site is of interest as dry season evapotranspiration appears to not be limited by soil moisture deficits, as demonstrated by eddy covariance data (Carswell et al., 2002), leaf hydraulics data (Fisher et al., 2006) and sap flow measurements (Fisher et al., 2007). At the Manaus site, soil hydraulics data (Tomasella and Hodnett, 1996) and evapotranspiration data (Malhi et al., 1998) have previously been collected and are used here for comparison.

First, rainfall patterns and atmospheric demand at Caxiuanã and Manaus were analysed to detect whether climatic differences between the sites could account for the differences in dry season evapotranspiration behaviour. Simple models of potential evapotranspiration and of soil water deficit were constructed – to estimate how much water must be supplied by the soil to allow unrestricted evapotranspiration to continue – under the different climate regimes. The use of a model allowed comparisons to be made between the climatic regimes in different sites and for different years.

Secondly, the soil water storage capacity was compared between the two sites. The amount of water which is available for evapotranspiration during a dry season depends fundamentally on the amount of water stored in the soil that is available to plants. Total soil water availability depends upon the volume of soil accessed by roots, and upon the amount of water available to plants per unit volume of accessed soil (the water holding capacity). The latter is a function both of plant rooting density and the soil hydraulic properties, both of which will vary with depth (Sperry et al., 1998). The soil hydraulic properties of relevance are the water retention capacity of the soil (how much water is held above the threshold for plant extraction) and the unsaturated hydraulic conductivity, which determines the rate of movement from the soil matrix to the root surface. Both water retention and soil hydraulic conductivity data are presented in this paper. The hydraulic conductivity data presented here are only the second published set of unsaturated hydraulic conductivity data for Amazonian soils. To allow the use of these soil properties in dynamic models of soil water movement, the parameters of the van Genuchten soil hydraulic model (van Genuchten, 1980) are calculated. In this paper we present new soil hydraulics data from an area where data are very sparse, and attempt to explain the differences in the observed results of existing gas exchange measurements between two contrasting sites in Amazonia, understanding of which is currently absent. Ultimately, better understanding of how climatic and edaphic factors combine to alter the rainforest responses to low soil moisture will allow more detailed predictions of which areas of Amazonia are most vulnerable to climatic change.

---

## 2. Materials and methods

### 2.1. Prediction of soil water deficit

It is frequently assumed that the approximate atmospheric demand over a month in a rainforest ecosystem is 100 mm (Sombroek, 2001; Malhi and Wright, 2004) and months with less rainfall than demand will need to utilise stored soil water.

However, this basic index does not account for the difference in the severity of dry periods beyond this threshold, and assumes that evaporative demand does not vary between seasons. Instead of assuming an atmospheric demand of  $100 \text{ mm month}^{-1}$ , a model was constructed to predict daily forest potential evapotranspiration under well-watered conditions. The method used was similar to that of Williams et al. (1997), who constructed an 'aggregated canopy model' (ACM) of daily carbon uptake, by fitting a simple empirical model to match the outputs of a detailed, well verified, half-hourly model of forest gas exchange, the soil-plant-atmosphere model (SPA, Williams et al., 1996, 1998, 2001). In this study, a model of potential evapotranspiration (PET) for Amazon forests (ACM-ET) was developed. The SPA model was used to generate a response surface of PET to radiation, temperature and vapour pressure deficit under a subset of observed Amazonian meteorological conditions. 2503 days of meteorological inputs to the SPA model were assembled using data from four sites across the Amazon basin: Tapajós, Caxiuanã, Manaus and Rondônia. The precise location and methodologies of the data collection are described elsewhere (Malhi et al., 1998; von Randow et al., 2004; Carswell et al., 2002; Saleska et al., 2003). Using a heuristic process, a simple set of equations was constructed to capture this response surface. A finite difference gradient optimisation routine was used to adjust the parameters of the equations so as to minimise the RMSE of the SPA vs. ACM-ET comparison of daily potential evapotranspiration (UMINF, IMSL Math Library). For model structure and inputs, see Appendix A.

To assess how the balance of PET and rainfall affects the demand for soil water, a dynamic model of soil moisture deficit was implemented. The maximum possible soil water deficit is predicted, assuming no reduction in evapotranspiration caused by low soil moisture. This is to estimate how much water the soil must provide for the canopy to continue to function normally, with no hydraulic restriction. The soil moisture deficit is assumed to initially be zero, as the simulation is started in the late wet season. Each month, water is removed from the soil according to the outputs of the ACM-ET model ( $E_t$ , in mm), and the monthly rainfall total ( $R_t$ , in mm) is added to the soil. The cumulative soil water deficit, CWD (mm) is altered by the difference between these values. If the CWD is positive at the end of the month then it is reset to zero as the excess rain is assumed to contribute to groundwater, hence soil water storage is ignored:

$$\text{CWD}_{t+1} = \text{CWD}_t + R_t - E_t \quad (1)$$

If  $\text{CWD}_t > 0$  then  $\text{CWD}_t = 0$

To estimate evaporative demand, the ACM-ET model was driven with daily meteorological data derived from Malhi et al. (1998) for Manaus, in 1995–96, the period when eddy covariance measurements were made, and from Fisher et al., 2007 for Caxiuanã in 2002–03, the period when sap flow measurements were made. The results were summed into monthly values. The aim here is to analyse, for these two sets of observations, whether soil or climate is the likely driver of the differences in dry season behaviour. Because only limited temporal ranges of meteorological and flux data are available at each site, these results do not necessarily

typify the average responses of these two sites to dry season rainfall. Instead, the analysis indicates whether soil or climate is a more likely driver of the inter-site differences in the years in question.

## 2.2. Measurement of soil hydraulic properties

### 2.2.1. Site

The experimental site is located at Caxiuanã National Forest, Pará, Brazil ( $1^\circ 43' 3.5'' \text{S}$ ,  $51^\circ 27' 36'' \text{W}$ ), a lowland *terra firme* rainforest. The soil is a yellow oxisol (Brazilian classification latosol), with a 0.3–0.4 m thick stony layer present between 3 and 4 m depth. The texture of the surface soil is 75–83% sand ( $>0.05 \text{ mm}$  particle diameter), 12–19% clay ( $<0.02 \text{ mm}$ ) and 6–10% silt (0.05–0.02 mm) (Ruivo and Cuhna, 2003). The surface soil consists of quartz in the sand fraction and predominantly kaolin in the clay fraction (Ruivo and Cuhna, 2003). Root biomass has been detected at this site at depths of 10 m (the deepest measurements made) (Fisher et al., 2007).

The area of forest investigated was delineated by the boundaries of the LBA (Large-Scale Biosphere–Atmosphere Experiment in Amazonia) Ecology Program (Avisar and Nobre, 2002) throughfall exclusion experiment (Fisher et al., 2006). The experiment covered a  $100 \text{ m} \times 200 \text{ m}$  area 500 m distant from the research station. The plot described shall hereafter be referred to as the 'experimental site'. All the experiments and sample collections occurred within this site, with the exception of the instantaneous profile experiment (see below), which occurred at a site 200 m closer to the research station.

### 2.2.2. Water retention curve measurement

Pressure plate analyses were conducted on intact samples, collected in April 2002 inside 55 mL soil cores, at depths corresponding to soil horizons identified by Ruivo and Cuhna (2003) in four 5 m deep soil trenches within the experimental site. Water contents were gravimetrically determined at  $-6$ ,  $-10$ ,  $-30$ ,  $-100$  and  $-1500 \text{ kPa}$ . The water retention curve for tensions between  $-8 \text{ kPa}$  and  $-1 \text{ kPa}$  was determined by *in situ* measurements of soil water potential ( $\psi$ ) and soil water content ( $\theta$ ) by the instantaneous profile method (IPM) described above. For the top metre of soil the two data sets were combined to give continuous water retention curves between  $-1$  and  $-1500 \text{ kPa}$  for each of the four soil depths (Fig. 1).

### 2.2.3. Unsaturated hydraulic conductivity measurement

In this study, hydraulic conductivity was measured only at tensions wetter than field capacity, due to logistical difficulties associated with measurement of drier soils. Two field based methods were used, tension infiltrometry (Ankeny et al., 1991) and the instantaneous profile method (Dirksen, 2000) to obtain estimates of  $K$  over different ranges of tension.

Firstly, measurements of unsaturated conductivity of soils in the macropore region ( $-0.05$  to  $-1 \text{ kPa}$  tension) were made using a tension infiltrometer (TI) with a 0.2 m disk (Soil Measurement Systems, Tucson, AZ, USA). Measurements of infiltration rates were made for every 0.1 kPa of tension between  $-0.05$  and  $-1 \text{ kPa}$ . It is necessary to correct the TI measurements for the increase in apparent flow caused by

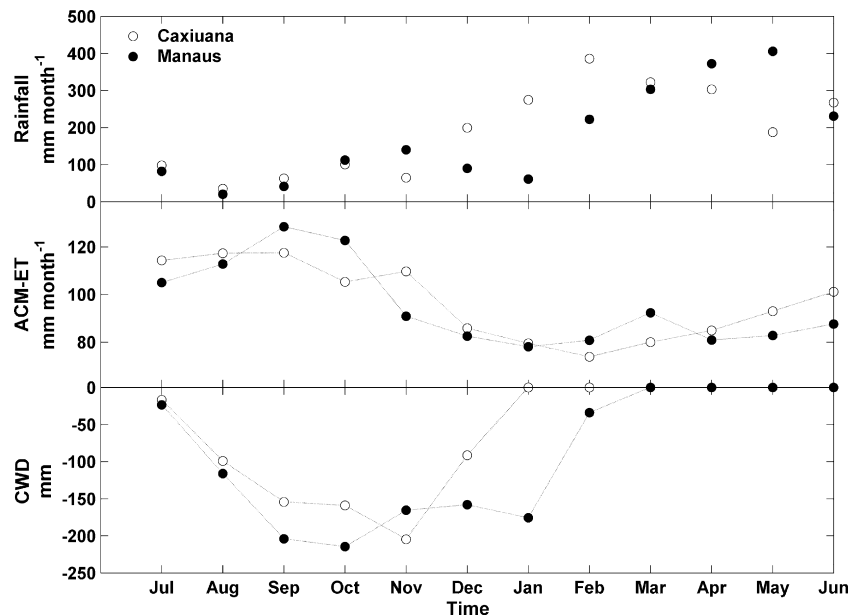


**Fig. 1 – Water retention curve data for four depths within the first metre of soil from pressure plates and *in situ* measurements, plus model approximations to the data made using the van Genuchten (VG) model. Error bars are ranges of samples taken from two different soil access shafts.**

three-dimensional capillary flow. To achieve this, correction method suggested by Reynolds and Elrick (1991) was applied. Eight hydraulic conductivity ( $K$ ) vs. water potential ( $\psi$ ) curves were measured using TI on the surface soil. Measurements were randomly located within the experimental site. Constraints to the random selection were that each sample site was at least 0.5 m from any tree more than 0.1 m in diameter, and at least 0.5 m from the edge of the plot or walkways within the plot, to avoid disturbed soil. In addition, three TI measurement profiles were made by removing the soil sequentially and measuring  $K$  vs.  $\psi$  at four different depths (0.1, 0.35, 0.5 and 0.9 m). The tension infiltrometer measurements for each profile were not located immediately below one another to prevent possible impacts of compaction of the soil column by the instrument.

Secondly, the instantaneous profile method was used to make measurements between  $-1$  kPa and  $-8$  kPa. The IPM is designed to measure the vertical flow of water through soil by isolating a column of soil, 1 m diameter by 1 m depth and wrapping it in plastic sheeting to prevent lateral water movement. Soil water content and water potential were measured at 0.05, 0.3, 0.6 and 0.9 m using CS615 TDR (time domain reflectometry) probes (Campbell Scientific, Loughborough, UK) and mini-tensiometers (Skye Instruments, Llan-drindod Wells, Wales), respectively, and readings were logged each minute using a Campbell Scientific CR10X datalogger (Campbell Scientific, Loughborough, UK). Water was poured on top of the monolith until the mini-tensiometers gave readings wetter than  $-0.2$  kPa for 5 min, indicating that near-saturation conditions had been achieved. The monolith was covered to prevent evaporation from the soil surface, and allowed to drain. The flow past the sensors ( $q$ ) was calculated at each depth as the loss in storage of the soil above the sensor in  $\text{mm h}^{-1}$ . Using this estimate, the hydraulic conductivity  $K$

( $\text{mm h}^{-1}$ ) was calculated using the method of Dirksen (2000) as:

$$K[\theta, z, t] = \frac{q[z, t]}{dH/dz[z, t]} \tag{2}$$

where  $z$  is depth (mm),  $t$  is time (h), and  $H$  is the hydraulic head (mm). The tensiometers, located at the same depth as the CS615 probes, also allowed the construction of *in situ* water retention curves. The monolith was left to drain until the water potential of each sensor was below  $-8$  kPa. The methods used were similar to those of Tomasella and Hodnett (1996), with the exception that, in this case, automatic TDR probes were used, rather than the neutron probe used in the Tomasella and Hodnett study, and the space of the probes was altered as a result. The maximum difference between the IPM and tension infiltrometry data was  $0.6 \text{ mm h}^{-1}$ , so continuous  $K$  vs.  $\psi$  relationships between  $-0.05$  and  $-8$  kPa were constructed for each depth using these two data sets (Fig. 4).

In the sandy soil at the Caxiuana site, the applicability of the calibration functions of the CS615 soil moisture sensors used in the IPM method was unknown, so a gravimetric calibration was conducted to assess how the sensors responded to varying soil moisture in the sandy latosol soil. Three 0.3 m long, 0.15 m diameter cores of soil were removed and kept intact within PVC piping. Two cores were taken from the surface soil (0.05–0.35 m depth) and one from 0.35 to 0.65 m depth. The locations were chosen at random (avoiding large roots) within the experimental site.

Each core was instrumented with a CS615 probe and a mini-tensiometer. The cores were continuously saturated until the automatic CS615 readings were stable for 30 min, and the mini-tensiometer readings were less than  $-0.02$  kPa. The cores were allowed to drain and placed inside a light box at ( $\sim 60^\circ \text{C}$ ) and simultaneous measurements of soil mass

and moisture sensor output were made at gradually increasing time intervals for ten days. At the end of the calibration period, the sensors were removed, and the cores were dried for 24 h at 105 °C and weighed to determine the mass of the dry soil.

Soil calibration curves were established by calculation of the volumetric water content  $\theta$  ( $\text{m}^3 \text{m}^{-3}$ ) using the following relationship:

$$\theta = \frac{M_w - M_d}{\rho V} \quad (3)$$

where  $M_w$  and  $M_d$  are the masses of the wet and dry soils, respectively (kg) and  $\rho$  is the density of water ( $\text{kg m}^{-3}$ ) and  $V$  is the volume of the core in  $\text{m}^3$ . This method is similar to that employed by Veldkamp and O'Brien (2000) to calibrate the same sensors for a soil in Ecuador.

#### 2.2.4. Soil hydraulic model parameterisation

Given the difficulties inherent in the measurement of unsaturated hydraulic conductivity, for most applications, soil hydraulic models are used to extrapolate the  $K_{\text{unsat}}$  data into drier soils. To facilitate this, the parameters of the van Genuchten (1980) model of soil hydraulic behaviour were estimated for the top metre of soil (see Appendix B). To allow comparison between the measurements, the data were grouped into four 0.1 m depth range categories. The depth categories used were 0.05–0.15 m, 0.25–0.35 m, 0.55–0.65 m and 0.85–0.95 m. By grouping together the data in this way it is assumed that each 0.1 m depth range is effectively homogeneous. This assumption is necessary because it is not practically possible to do all the measurements in the same location.

The van Genuchten model required parameter optimisation. This was achieved using the simplex search method (Lagarias et al., 1998) embedded in 'Matlab' (MathWorks Inc.,

Natick, MA, USA). The parameters were fitted to minimise the error parameter  $e$ , the sum of the relative root mean square error between the observed and modelled water contents ( $\theta_o$  and  $\theta_m$ ) plus the sum of the relative root mean square errors between log of the  $K$  data ( $K_o$ ) and the log of the model  $K$  prediction ( $K_m$ )

$$e = \sum \frac{\theta_o - \theta_m}{\theta_o} + \sum \frac{\log K_o - \log K_m}{\log K_o} \quad (4)$$

The log transformation of  $K$  is based on the assumption that the data error is constant on a log scale, and avoids bias of the fitting routine towards the larger values, as  $K$  varies over many orders of magnitude. van Genuchten parameters were not fitted to the data from the lower layers where only pressure plate data was available, as the sample size was too low to constrain all the parameters of the model.

## 3. Results

### 3.1. Predicted soil water deficit

During the respective measurement periods, the Caxiuanã site received more rainfall in total ( $2350 \text{ mm year}^{-1}$ ) than the Manaus site ( $2088 \text{ mm year}^{-1}$ ). Both sites experienced strong seasonality in rainfall, with wet season rainfall peaking around 400 mm per month in February at Caxiuanã and in May at Manaus (Fig. 2). Low rainfall began in July in both sites (115 mm at Caxiuanã and 82 mm at Manaus). The driest month in both cases was August, however, the dry season at Caxiuanã lasted until December, whereas at Manaus high rainfall ( $>100 \text{ mm}$ ) only returned in February. Both the wet and dry season rainfall at Manaus was close to the long-term average for Manaus City (Harris et al., 2004), and the Caxiuanã rainfall was 5 mm (1%) less in the dry season and 80 mm (5%)

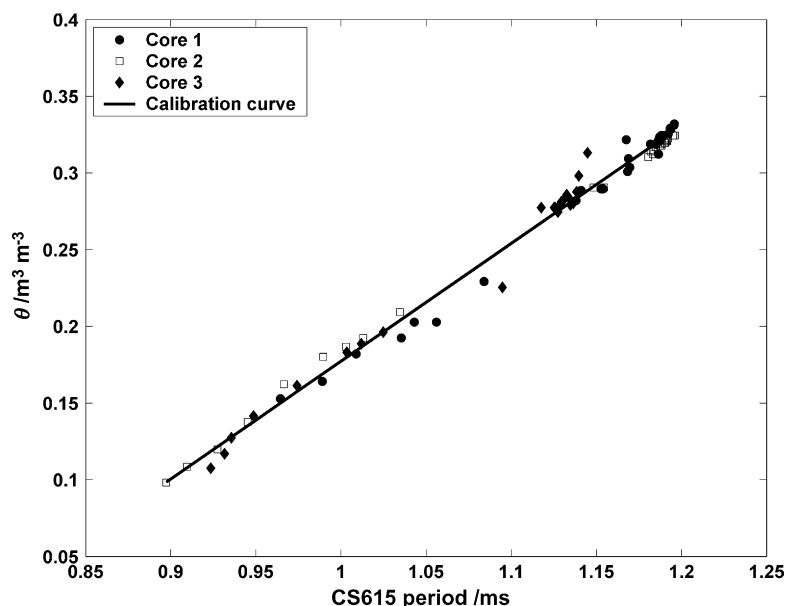


Fig. 2 – Comparison of rainfall (squares), modelled potential evapotranspiration (diamonds) and estimated cumulative water deficit (circles, CWD) at Caxiuanã (open symbols) and Manaus (filled symbols).

less in the wet season than the average over 5 years of measurements at Caxiuanã.

The simple model predicted seasonality in the monthly potential evapotranspiration, ranging at both sites from 120 to 130 mm in the dry season to 70–80 mm in the wet season. The data are from different years, but the seasonal cycle is similar between sites, with a slightly greater PET at Caxiuanã in November, and lower in September and October.

The longer dry season at Manaus did not create a larger soil moisture deficit than at Caxiuanã. Partly because there was a ‘mini’ wet season in November, when the soil moisture was slightly recharged, according to the simple model, and partly because atmospheric demand was relatively low between November and February. The maximum predicted seasonal water deficit was similar in the two forests; –210 mm at Caxiuanã and –214 mm at Manaus. The model results thus indicate that there were not large differences in maximum demand for soil moisture between the two sites. The water deficit was maintained for one month longer in Manaus than in Caxiuanã.

### 3.2. Soil hydraulic properties

#### 3.2.1. Soil moisture sensor calibration

The responses of the CS615 probes to water content were effectively linear. There was little variation between the cores, so all the data were grouped together to produce the following calibration equation:

$$\theta = 0.79P - 0.59 \quad (r^2 = 0.79) \quad (5)$$

where  $\theta$  is the volumetric water content ( $\text{m}^3 \text{m}^{-3}$ ) and  $P$  is the period output of the CS615 sensors in ms (Table 1).

#### 3.2.2. Water retention curves

The data describe a sigmoidal relationship when plotted on a log–log scale, and give a good fit to the van Genuchten model (RMS error =  $0.013 \text{ m}^3 \text{m}^{-3}$ ,  $r^2 = 0.88$  to  $0.98$ ). The van Genuchten parameters used to interpolate the relationship are shown

in Table 2. The soil water content at –1500 kPa is very low ( $0.07$  to  $0.15 \text{ m}^3 \text{m}^{-3}$ ) due to the low clay content. The water retention curves were not measured between saturation and –1 kPa so the water released at these tensions is unknown.

The water retention curves for the deeper soil layers (between 1.0 and 4.5 m depth, Fig. 3) were similar to those of the top metre of soil in that the amount of water released between –6 and –1500 kPa was within the range found in the top metre ( $0.164$  to  $0.243 \text{ m}^3 \text{m}^{-3}$ ). The variation in absolute water content in the pressure plate data was greater than the variation detected in the IPM as it included both spatial and vertical heterogeneity. Only one profile was measured for the IPM, so the effect of spatial variation was not known.

#### 3.2.3. Hydraulic conductivity

The hydraulic conductivity data (Fig. 4) showed good agreement between the two hydraulic conductivity measurement techniques (tension infiltrometry and instantaneous profiling) where their ranges overlapped at –1 kPa. The observed values of  $K$  varied over ~5 orders of magnitude over the measured range of water contents, between  $844$  and  $0.01 \text{ mm h}^{-1}$ . The van Genuchten model, which was simultaneously fitted against the water retention curve and the conductivity data, is generally a good descriptor of the shape of the  $K$  vs.  $\psi$  data (RMS error =  $0.168$ – $0.33 \log_{10} \text{ mm h}^{-1}$ ,  $r^2 = 0.875$  to  $0.998$ ), but there is some deviation of the model away from the data as saturation is approached at –0.05 kPa. Here the  $K$  data are on average  $367 \text{ mm h}^{-1}$  higher than the model predictions. High  $K$  values close to saturation potentially indicate the existence of secondary system of large soil pores. These features were also observed by Tomasella and Hodnett (1996) for rainforest soils, and were hypothesized to be due to the effect of biogenic macropores (Chauvel et al., 1991), which substantially increase the maximum hydraulic conductivity of the soil matrix. The van Genuchten model assumes a uni-modal pore size distribution and thus is not able to predict the effects of such secondary pore systems.

**Table 1 – Summary of the available soil hydrology data at the Caxiuanã site**

Data type	$\psi$ range (kPa)	Depth range (m)	K data	$\psi$ data	$\theta$ data
Tension infiltrometer	–0.05 to –1	0–0.9	Yes	Yes	No
Pressure plates	–6 to –1500	0–4.5	No	Yes	Yes
Soil calibration cores	–0.1 to –6	0–0.9	No	No	Yes
Instantaneous profile method	–0.8 to –8	0–0.9	Yes	Yes	Yes

**Table 2 – van Genuchten parameters for four soil depths at the Caxiuanã site**

Model	Parameter	Depth (m)			
		0.50–0.15	0.25–0.35	0.45–0.55	0.90–0.10
van Genuchten	$\theta_r$	0.127	0.027	0.022	0.105
	$\theta_s$	0.516	0.421	0.384	0.413
	$\alpha$	5.40	1.27	1.82	2.10
	$N$	1.27	1.23	1.10	1.20
	$K_{\text{sat}}$	1011	1545	3102	2123
	$l$	–1.25	1.88	–1.42	–1.03

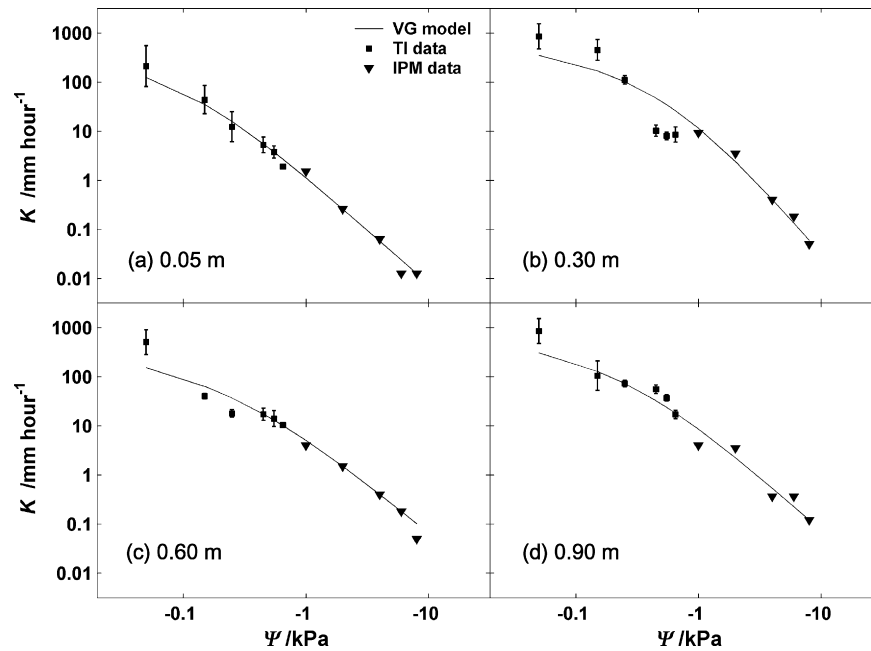


**Fig. 3 – Hydraulic conductivity data, from tension infiltrometer (TI) and instantaneous profiling (IPM), with model approximations to the data using the van Genuchten VG model for four depths within the first metre of soil. Error bars are standard deviations of four independent tension infiltrometer samples.**

3.2.4. *Comparison of soil properties at caxiuanã and manaus*  
 The Caxiuanã soil data were compared to the data collected at a site near Manaus by Tomasella and Hodnett (1996). The Caxiuanã and Manaus soils differed significantly in terms of absolute water content. The Caxiuanã soil had lower soil water content across all tensions (*t*-test *p* value <0.01), with the maximum measured water content being  $0.37 \text{ m}^3 \text{ m}^{-3}$  compared to  $0.52 \text{ m}^3 \text{ m}^{-3}$  at Manaus (Tomasella and Hodnett, 1996). This is to be expected, as clay soils hold more water at very low tensions (<1500 kPa) in their microporous structure. However, the sandy soil at Caxiuanã had a much greater range of water content over the range of tensions measured. The water held in the soil within the range available to plants was

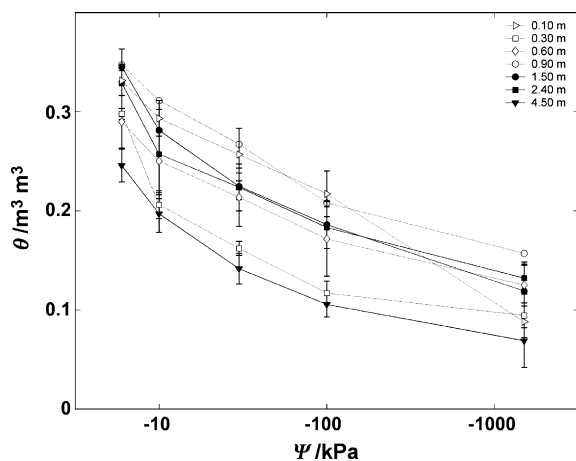


**Fig. 4 – Soil water retention curves of all soil layers derived from pressure plate analyses. Error bars correspond to ranges of samples from two different sites.**

estimated. It was assumed that water held between 0 and  $-6 \text{ kPa}$  is not available to plants, as it is quickly drained away after a rain event. The lower limit of water extraction is not known, as it depends upon root density and osmotic potential, soil texture and the capacity of plants to resist xylem embolism (Sperry et al., 1998). Therefore, the soils were compared for a wide range of possible extraction limits. The lower limit considered was  $-1500 \text{ kPa}$ , the commonly assumed ‘wilting point’, beyond which plants are not able to function (Nepstad et al., 2004). In a modelling study at Caxiuanã, Fisher et al. (2007) used measured root biomass profiles, among other data, to parameterise a model of forest gas exchange. This model, which was verified against soil water content data, predicted that in the top 5 m of soil, where roots were abundant, predicted extraction did occur down to  $-1500 \text{ kPa}$ . However, the lowest water potential predicted for soil layers between 5 and 10 m depth during two dry seasons, both of which exhibited very restricted forest water use, was  $\sim -100 \text{ kPa}$ . This wetter predicted extraction limit was mainly due to the low root density in these layers slowing the modelled rate of water extraction from the deep soils. We have therefore also analysed the water available between  $-6$  and  $-100 \text{ kPa}$  because this is the predicted amount of water available from deep layers under the prevailing climatic and biological circumstances.

At Manaus, available water content between  $-6 \text{ kPa}$  and  $-100 \text{ kPa}$  averaged across all the layers tested was  $0.040 \pm 0.016 \text{ m}^3 \text{ m}^{-3}$  (Tomasella and Hodnett, 1996). Data were not available for soils drier than  $-100 \text{ kPa}$ , but extrapolation of the van Genuchten curves predicts that there was an average of  $0.045 \pm 0.011 \text{ m}^3 \text{ m}^{-3}$  released between  $-100 \text{ kPa}$  and  $-1500 \text{ kPa}$  making a total of  $0.095 \pm 0.027 \text{ m}^3 \text{ m}^{-3}$ . At Caxiuanã, the average water released between  $-6 \text{ kPa}$  and

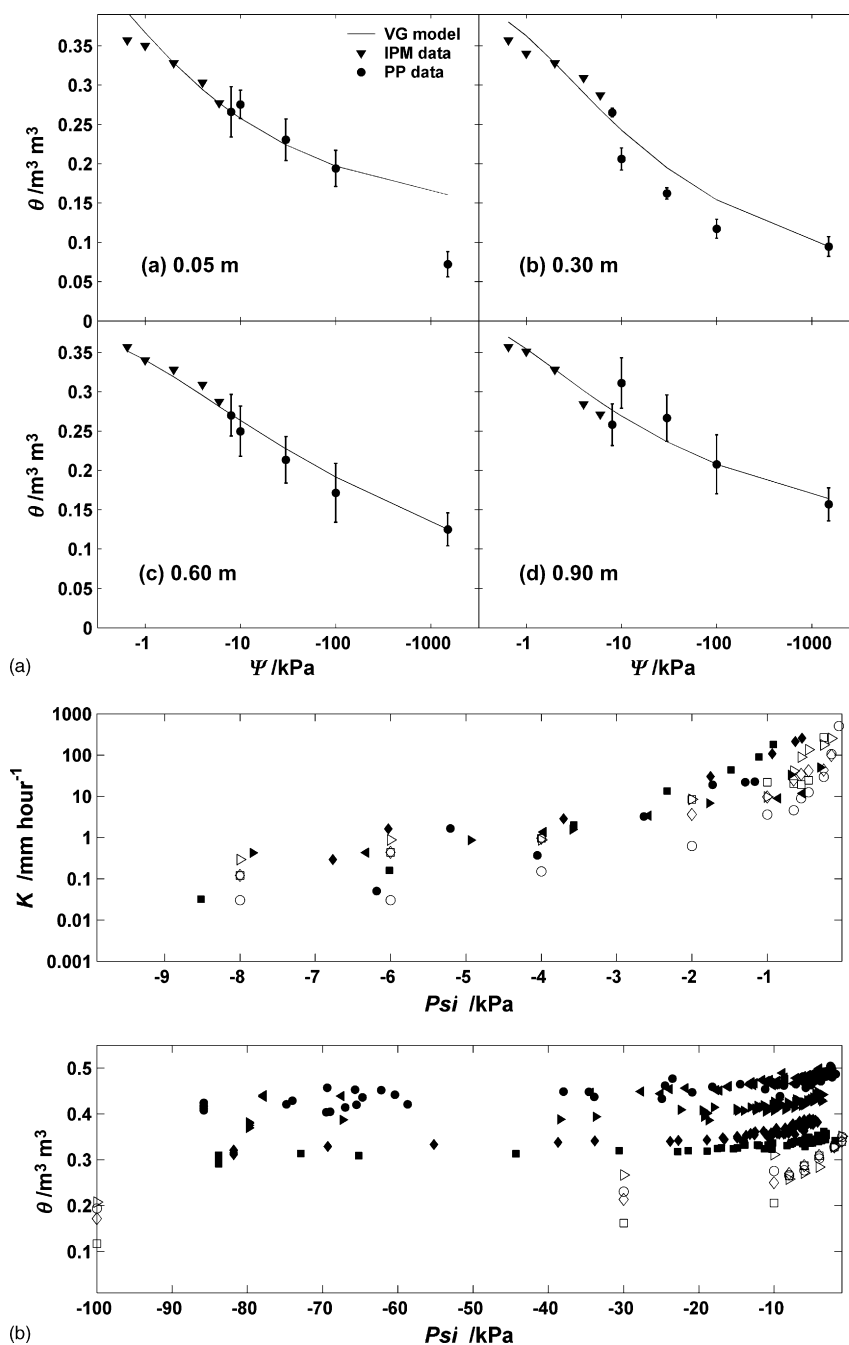


**Fig. 5 – (a) Comparison of IPM data from Manaus (closed symbols) and Caxiuanã (open symbols). Caxiuanã data: 0.05 m = circles, 0.30 m = squares, 0.60 m = diamonds, 0.90 m = triangles. Manaus data: 0.30 m = circles, 0.50 m = squares, 0.75 m = diamonds, 1.05 m = right pointing triangles, 1.35 m = left pointing triangles. (b) Comparison of water retention curves from Manaus (closed symbols) and Caxiuanã (open symbols). Caxiuanã data: 0.05 m = circles, 0.30 m = squares, 0.60 m = diamonds, 0.90 m = triangles. Manaus data: 0.20 m = circles, 0.40 m = squares, 0.60 m = diamonds, 0.80 m = right pointing triangles, 1.00 m = left pointing triangles. Note the difference in scale between the plots.**

–100 kPa over the top metre of soil (to allow direct comparison with the Manaus data) was  $0.138 \pm 0.046 \text{ m}^3 \text{m}^{-3}$  and that between –100 kPa and –1500 kPa was  $0.062 \pm 0.034 \text{ m}^3 \text{m}^{-3}$ , giving a total of  $0.200 \pm 0.032 \text{ m}^3 \text{m}^{-3}$ . Therefore, if the limit of extraction is –100 kPa, then the Caxiuanã soil holds 3.4 times more water than Manaus. If it is –1500 kPa, the Caxiuanã soil holds 2.1 times as much as the Manaus soil.

The relationship between water potential  $\Psi$  and unsaturated conductivity  $K$ , was similar (t-test  $p$  value = 0.34) between the Manaus and Caxiuanã sites (Fig. 5) for the range of  $\Psi$  over which  $K$  was measured (–0.1 to –8 kPa) (this is for soils wetter than field capacity, and thus not the same range as that over which the plant available water was compared). We therefore expect that the rate of soil-to-root water transport at

a given  $\psi$  would be similar between the two sites, given similar rooting density.

#### 4. Discussion

The forest at Caxiuanã appears to be able to withstand the observed dry seasons without restriction on evapotranspiration caused by low soil moisture (Carswell et al., 2002; Fisher et al., 2006, 2007). In contrast, the forest at Manaus experienced substantial declines in evapotranspiration in the 1996 dry season, as measured by eddy covariance (Malhi et al., 1998). It is important to understand the reasons for these different behaviours as the current water limitation status of the forest is a key uncertainty in our ability to predict the magnitude of the proposed 'Amazon dieback' feedback mechanism (Cox et al., 2000; Friedlingstein et al., 2006). In this study, two abiotic factors which may potentially explain the differences between the two forest ecosystems were investigated; climate patterns and plant available soil water storage capacity. Neither the potential evapotranspiration nor rainfall patterns differed substantially between the two sites, leading to only small differences of only 7 mm in projected maximum soil water deficit. However, the available soil moisture at the Caxiuanã site was between 2.1 and 3.4 times greater per volume of soil than the Manaus soil, depending on the (unknown) 'limit' of water extraction. Therefore, we conclude that there is little evidence that climatic factors are the cause of restrictions to evapotranspiration in the dry season at Manaus, but there is some evidence to suggest that the very low plant available soil water storage capacity may make this forest more prone than the Caxiuanã forest to experiencing drought stress.

One unknown in this study is the difference in active root biomass profiles between sites. If the active roots at Manaus are substantially shallower than at Caxiuanã, and access a smaller volume of soil, then this may also contribute to the differences in water supply between sites. At Caxiuanã, water extraction has been observed down to 5.0 m (Fisher et al., 2007). Hodnett et al. (1996) observed water extraction down to at least 3.6 m depth at a site near Manaus. Both these studies detected soil water extraction at the maximum depth observed. The absence of measurements of soil water content below these depths means that the active rooting depth cannot be estimated. For this study, it is of course possible that very deep roots at Caxiuanã might be the reason for the dry season resilience. However, we know root and water uptake occurs down to at least 3.6 m at Manaus (Hodnett et al., 1996). At Caxiuanã, this rooting depth would easily provide enough water to cover the predicted soil water deficit of 210 mm (this depth of soil being predicted to provide between 496 and 720 mm, depending on the assumed uptake limit, but not allowing for changes in soil properties with depth), so rooting depth differences cannot easily explain the different responses.

Roots have been detected at 10 m depth at Caxiuanã, and at a number of other Amazonian sites (Nepstad et al., 1994; Moreira et al., 2000; Nepstad et al., 2004), but at very low density. It is not known how active these roots are in water uptake but some studies have suggested that deep roots

mainly improve plant water uptake capabilities via the use of hydraulic lift (Lee et al., 2005; Oliveira et al., 2005). This mechanism, whereby water is continuously transferred from wetter deep layers to drier shallow layers in the dry season, may help to overcome the limitations on water uptake caused by soil-to-root resistance, as this uptake mechanism acts all of the time, not just when the plant is transpiring. However, at the Manaus site, the existence of dry season hydraulic limitation potentially means that the impact of hydraulic lift is limited.

Despite the demonstrated existence of deep water extraction (Moreira et al., 2000; Bruno et al., 2006) and hydraulic lift (Oliveira et al., 2005) at the Tapajós rainfall exclusion experiment, Nepstad et al. (2007) found a three year delay between beginning a rainfall exclusion experiment and the onset of increased tree mortality and at least one year delay before the onset of leaf water stress and LAI changes (see Nepstad et al., 2002). The results from this rainfall exclusion experiment suggests that stored soil water at this site can buffer large changes in rainfall for a short period, but the long-term depletion of soil water reserves eventually causes limitations in water supply. This is important, as it means that the responses to short-term perturbations, like El Niño years, do not necessarily provide insight into the responses of the forest to long-term changes in water balance. Another rainfall exclusion experiment, also located at Caxiuanã (Fisher et al., 2007) responded by reducing evapotranspiration in response to the imposed drought in a single year, but this rainfall exclusion was imposed continuously throughout the year, not just in the wet season (Nepstad et al., 2002) so the results are not directly comparable (also, measurements of the gas exchange of the Tapajós drought experiment are not available for comparison using the methods employed in this study). Improved understanding of rooting behaviour and soil depth, along with improvements in soil hydraulic information, are necessary to disentangle the effects of abiotic soil properties and of rooting behaviour.

Another unknown is the lower tension limit of extraction of soil water. In this study, we have used two contrasting limits to investigate the consequences for our predictions of addressing this uncertainty. It is commonly assumed that plants may extract soil water down to  $-1500$  kPa, the 'wilting point' (Cox et al., 1998; Werth and Avissar, 2004). Recently, it was proposed using a modelling analysis that changes in water potential alone could not explain the patterns of gas exchange observed at Manaus, and that it was also necessary to invoke changes in soil-to-leaf hydraulic conductance to explain the predictions (Williams et al., 1998). This finding was supported by Fisher et al. (2007) using a model which predicted soil water uptake resistance 'a priori' from soil water content and root biomass profiles. An important implication of this proposed hydraulic resistance limitation mechanism is that the rate of water supply to leaves might be severely limited long before the absolute limit of extraction is reached and where roots are sparse, plant water use can be reduced at quite high water potentials. Therefore, to discuss 'limits' of water uptake is to some degree misleading, as transpiration may be reduced by slow water movement despite no absolute threshold of water content extraction having been reached. This was empirically demonstrated by Fisher et al. (2006) who found that sub-

stantial reduction in water use of canopy trees subjected to artificially reduced soil moisture occurred in the dry season at Caxiuanã, despite the existence of only slightly negative soil water potentials of  $-0.2$  to  $-0.6$  MPa. These water potentials were estimated from pre-dawn leaf water potential measurements, a proxy for the ‘average’ soil water potential of the profile, assuming the system is in hydraulic equilibrium. Furthermore, in the dry season, there was a large increase in the measured below-ground hydraulic resistance, supporting the hypothesis that below ground resistance to water transport could be severely limiting forest water use. Nevertheless, for the purposes of this paper, it is necessary to demonstrate that the soil properties at Caxiuanã and Manaus differ substantially in terms of water retention, so it is necessary to artificially impose a range for the available plant water content. Here we have used two extreme extraction limits, an upper and lower estimate. Soil water availability was substantially higher at Caxiuanã in both instances, so our findings are not affected by this uncertainty. In addition we extended the analysis to very low soil water potentials ( $-5000$  kPa, data not shown) to investigate the likelihood of water being released from the clay micropore matrix of the Manaus soil. This analysis predicted that, at Manaus there was less than 2% additional water extraction, and at Caxiuanã there was between 1.3 and 3.8% additional water extraction. This therefore supports rather than undermines the hypothesis that the Caxiuanã soil has higher plant available water.

If  $K$  is an important determinant of forest water use, via its impact on water transport, then it will be necessary eventually to predict it at a regional scale using an empirical model of soil properties. It is clear from the lack of data (Tomasella and Hodnett, 1997) on this important soil property (which is also necessary for infiltration and runoff modelling), that further investigation is an important priority for understanding Amazonian forest gas exchange processes.

The main conclusion of this study is that while there were no differences in total soil water deficit between the Manaus and Caxiuanã sites in the years considered for this analysis, there were very large differences in the water retention capacity of the soils. We suggest that the main factor driving the different behaviours is likely to be the very low soil water retention capacity of the clay oxisol at Manaus compared to the sandy oxisol at Caxiuanã. Some uncertainty remains surrounding the impact of deep roots and vegetation strategies regarding water stress avoidance. However, we believe that the scarcity of good soil hydraulics information for Amazonia remains an impediment to the creation of accurate models of biosphere–atmosphere exchange, particularly for the purpose of identifying which forest areas may be particularly sensitive to climatic change.

## Acknowledgements

The work presented in this paper would not have been possible without the input of the late Dr Wim Sombroek, and the authors would like to dedicate this paper to his memory.

In addition, we are grateful to Javier Tomasella and Martin Hodnett for many helpful comments on the manuscript and for the provision of soil hydraulics data from Manaus. This

work was supported by a University of Edinburgh Faculty Research Scholarship, several Natural Environment Research Council (UK) research grants, a Natural Resources International Foundation Fellowship. We would like to thank Edso Veldkamp for advice on soil moisture sensor calibration, Rafael Ferreira da Costa and Luiz Aragão for field assistance and the Museu Paraense Emilio Goeldi for the use of their field station and laboratory facilities.

## Appendix A. ‘ACM-ET’ Potential evapotranspiration model

Potential evapotranspiration was modelled as the product of the atmospheric demand and the surface conductance using a modified version of the Penman-Montieth equation (Jones, 1992).

$$D = \frac{p_1(s(I - p_2) + c_p g_a V \rho_a)}{s + \lambda(g_a/g_c)}$$

where  $I$  is average daily radiation ( $\text{Wm}^{-2}$ ),  $V$  is the average daily vapour pressure deficit (kPa), and  $g_c$  is surface conductance.  $\lambda$  is the psychrometric constant ( $0.066 \text{ kPa } ^\circ\text{C}^{-1}$ )  $c_p$  is the specific heat of air ( $1010 \text{ J Kg}^{-1} \text{ K}^{-1}$ ) and  $\rho$  is the density of air ( $1.2 \text{ Kg m}^{-3}$ ).  $p_1$  is a correction between the average daily radiation and the radiation observed.  $p_2$  is the intercept of the relationship between radiation and ET. These empirical fitting parameters are necessary because the Penman-Montieth is an instantaneous equation, but the input parameters are daily values.  $s$  is the change in slope of the vapour pressure curve with temperature,  $T$  (K):

$$s = 6.166 \frac{12.27T}{273.3 + T}$$

Surface conductance is defined as:

$$g_c = p_3 L \psi e^{p_4 \sqrt{R}}$$

where  $\psi$  is the difference between the minimum leaf water potential and the bulk soil water potential (MPa).  $R$  is the soil-to-leaf hydraulic resistance ( $\text{s m}^{-2} \text{ MPa mmol}^{-1}$ ) and  $L$  is the leaf area index ( $\text{m}^2 \text{ m}^{-2}$ ).  $g_s$  is increased by high LAI and  $\psi$  values, and is limited when both radiance and soil-to-leaf hydraulic resistance are high. This is because high irradiance is linked to high atmospheric demand. In times of low soil water availability, this tends to result in stomatal closure.  $p_3$  and  $p_4$  are further fitting parameters. The parameters were optimised to fit the evapotranspiration data from the output of the SPA model. These values include the effects of soil evaporation and leaf surface evaporation. The values of the fitted parameters as determined by the optimisation routine were:

$$p_1 = 2.74, p_2 = 6.22, p_3 = 4.7 \times 10^{-5}, p_4 = 3.0 \times 10^{-2}$$

The  $r^2$  value between the SPA model and the aggregated model was 0.87. The model residuals did not correlate with any of the input variables. The average relative model error was 12%. The SPA model output has been verified against sap flow data from both well watered and drought-stressed sap

flow data from Fisher et al. (2007). The ACM model was not compared directly to the data because of the discrepancy between the sap flow data and the evapotranspiration model output. To simulate well-watered conditions at the Manaus and Caxiuanã sites, the soil water supply parameters  $\psi$  and  $R$  were set to values which correspond to well-watered conditions (2.5 MPa and  $1.0 \text{ s m}^{-2} \text{ MPa mmol}^{-1}$ , respectively).

## Appendix B. van Genuchten soil hydraulic properties model

The van Genuchten (1980) model describes the water release curve as:

$$S_e = \frac{\theta - \theta_r}{\theta_s - \theta_r} = [1 + (\alpha\psi)^n]^{1-1/n}$$

where  $S_e$  is the effective saturation,  $\theta$  is the soil water content and with  $\theta_s$  and  $\theta_r$  as the saturated and residual soil water contents respectively ( $\text{m}^3 \text{ m}^{-3}$ ),  $\alpha$  is a scaling factor which determines the maximum pore size ( $\text{kPa}^{-1}$ ), and  $n$  is a dimensionless curve shape parameter. Hydraulic conductivity  $K$  ( $\text{mm h}^{-1}$ ) is given as;

$$K = K_{\text{sat}} \frac{(1 - (\alpha\psi)^{n-1} [1 + (\alpha\psi)^n]^{-(1-1/n)})^2}{[1 + (\alpha\psi)^n]^{1-1/n}}$$

where  $K_{\text{sat}}$  is the saturated hydraulic conductivity ( $\text{mm h}^{-1}$ ). A 'tortuosity factor'  $l$ , is required, to account for the influence of soil structure on conductivity. Therefore the shapes of the water retention and hydraulic conductivity curves are independent.

## REFERENCES

- Ankeny, M.D., Ahmed, M., Kaspar, T.C., Horton, R., 1991. A simple field method for determining unsaturated hydraulic conductivity. *Soil Sci. Soc. Am. J.* 55, 467–470.
- Araújo, A.C., Nobre, A.D., Kruijt, B.J., Elbers, A., Dallarosa, R., Stefani, P., von Randow, C., Manzi, A.O., Culf, A.D., Gash, J.H.C., Valentini, R., Kabat, P., 2002. Comparative measurements of carbon dioxide fluxes from two nearby towers in a central Amazonian rainforest: The Manaus LBA site. *J. Geophys. Res.-Atmos.* 107 (D20), 8090.
- Avissar, R., Nobre, C.A., 2002. Preface to special issue on the Large-Scale Biosphere-Atmosphere Experiment in Amazonia (LBA). *J. Geophys. Res.-Atmos.* 107 (D20), 8034.
- Bruno, R.D., da Rocha, H.R., de Freitas, H.C., Goulden, M.L., Miller, S.D., 2006. Soil moisture dynamics in an eastern Amazonian tropical forest. *Hyd. Proc.* 20, 2477–2489.
- Carswell, F.E., Costa, A.L., Palheta, M., Malhi, Y., Meir, P., Costa, J.D.R., Ruivo, M.L.P., Leal, L.D.M., Costa, J.M.N., Clement, R.J., Grace, J., 2002. Seasonality in CO<sub>2</sub> and H<sub>2</sub>O flux at an eastern Amazonian rainforest. *J. Geophys. Res.-Atmos.* 107 (D20), 8076.
- Chauvel, A., Grimaldi, M., Tessier, D., 1991. Changes in soil pore-space distribution following deforestation and revegetation – an example from the central Amazon basin. *Brazil. Forest Ecol. Manage.* 38, 259–271.
- Cox, P.M., Huntingford, C., Harding, R.J., 1998. A canopy conductance and photosynthesis model for use in a GCM land surface scheme. *J. Hydrol.* 212/213, 79–94.
- Cox, P.M., Betts, R.A., Jones, C.D., Spall, S.A., Totterdell, I.J., 2000. Acceleration of global warming due to carbon-cycle feedbacks in a coupled climate model. *Nature* 408, 184–187.
- Cox, P.M., Betts, R.A., Collins, M., Harris, P.P., Huntingford, C., Jones, C.D., 2004. Amazon dieback under climate-carbon cycle projections for the 21st Century. *Theor. Appl. Climatol.* 78 (1–3), 177–185.
- da Rocha, H.R., Goulden, M.L., Miller, S.D., Menton, M.C., Pinto Ldvo, de Freitas, H.C., Figueira Ames, 2004. Seasonality of water and heat fluxes over a tropical forest in eastern Amazonia. *Ecol. Appl.* 14 (4), S22–S32.
- Dirksen, C., 2000. Unsaturated hydraulic conductivity. In: Smith, K.E., Mullins, C.E. (Eds.), *In Soil and Environmental Analysis: Physical Methods*. second ed. Marcel Dekker, Inc., New York, pp. 183–237.
- Fisher, R.A., Williams, M., Lobo do Vale, R., Costa, A., Meir, P., 2006. Evidence from Amazonian forests is consistent with isohydric control of leaf water potential. *Plant Cell Environ.* 29 (2), 151–165.
- Fisher, R.A., Williams, M., da Costa, A.L., Malhi, Y., da Costa, R.F., Almeida, S., Meir, P.W., 2007. The response of an Eastern Amazonian rainforest to drought stress: Results and modelling analyses from a through-fall exclusion experiment. *Glob. Change Biol.* 13, 1–8.
- Friedlingstein, P., Cox, P.M., Betts, R.A., Bopp, L., von Bloh, W., Brovkin, V., Cadule, P., Doney, S., Eby, M., Fung, I., Bala, G., John, J., Jones, C., Joos, F., Kato, T., Kawamiya, M., Knorr, W., Lindsay, K., Matthews, H.D., Raddatz, T., Rayner, P., Reick, C., Roeckner, E., Schnitzler, K.-G., Schnur, R., Strassmann, K., Weaver, A.J., Yoshikawa, C., Zeng, N., 2006. Climate-carbon cycle feedback analysis, results from the C4MIP model intercomparison. *J. Climate* 19 (14), 3337–3353.
- Goulden, M.L., Miller, S.D., da Rocha, H.R., Menton, M.C., de Freitas, H.C., Figueira Ames, de Sousa, C.A.D., 2004. Diel and seasonal patterns of tropical forest CO<sub>2</sub> exchange. *Ecol. Appl.* 14 (4), S42–S54.
- Grace, J., Malhi, Y., Lloyd, J., McIntyre, J., Miranda, A.C., Meir, P., Miranda, H.S., 1996. The use of eddy covariance to infer the net carbon dioxide uptake of Brazilian rainforest. *Glob. Change Biol.* 2 (3), 209–217.
- Harris, P.P., Huntingford, C., Gash, J.H.C., Hodnett, M.G., Cox, P.M., Malhi, Y., Araujo, A.C., 2004. Calibration of a land-surface model using data from primary forest sites in Amazonia. *Theor. Appl. Climatol.* 78 (1–3), 27–45.
- Hodnett, M.G., Oyama, M.D., Tomasella, J., Marques Filho, A.de.O., 1996. Comparisons of long-term soil water behaviour under pasture and forest in three areas of Amazonia. In: Gash, J.H.C., Nobre, A.D., Roberts, J.M., Victoria, R.L. (Eds.), *Amazonian Deforestation and Climate*. Wiley, Chichester, UK, pp. 57–77.
- Huete, A.R., Didan, K., Shimabukuro, Y.E., Ratana, P., Saleska, S.R., Hutyra, L.R., Yang, W., Nemani, R.R., Myneni, R., 2006. Amazon rainforests green-up with sunlight in dry season. *Geophys. Res. Lett.* 33. (6), L06405.
- Huntingford, C., Harris, P.P., Gedney, N., Cox, P.M., Betts, R.A., Marengo, J.A., Gash, J.H.C., 2004. Using a GCM analogue model to investigate the potential for Amazonian forest dieback. *Theor. Appl. Climatol.* 78 (1–3), 177–185.
- IPCC Fourth Assessment Report, 2007. Summary for Policymakers: Climate Change. The Physical Science Basis.
- Jones, H.G., 1992. *Plants and Microclimate*. Cambridge University Press, Cambridge.
- Lagarias, J.C., Reeds, J.A., Wright, M.H., Wright, P.E., 1998. Convergence properties of the Nelder-Mead Simplex Method in low dimensions. *Siam J. Optimiz.* 9 (1), 112–147.
- Lee, J.E., Oliveira, R.S., Dawson, T.E., Fung, I., 2005. Root functioning modifies seasonal climate. *Proc. Natl Acad Sci.* 102 (49), 17576–17581.

- Malhi, Y., Nobre, A.D., Grace, J., 1998. Carbon dioxide transfer over a central Amazonian rainforest. *J. Geophys. Res.-Atmos.* 103, 31.593–31.612.
- Malhi, Y., Pegoraro, E., Nobre, A.D., Pereira, M.G.P., Grace, J., Culf, A.D., Clement, R., 2002. Energy and water dynamics of a central Amazonian rainforest. *J. Geophys. Res.-Atmos.* 107 (D20), 8061.
- Malhi, Y., Wright, J., 2004. Spatial patterns and recent trends in the climate of tropical forest regions. *Philos. T. R. Soc. B.* 359, 311–329.
- Moreira, M.Z., Sternberg, L.D.L., Nepstad, D.C., 2000. Vertical patterns of soil water uptake by plants in primary forest and abandoned pasture in the eastern Amazon: an isotopic approach. *Plant Soil* 222, 95–107.
- Nepstad, D.C., Decarvalho, C.R., Davidson, E.A., Jipp, P.H., Lefebvre, P.A., Negreiros, G.H., Dasilva, E.D., Stone, T.A., Trumbore, S.E., Vieira, S., 1994. The role of deep roots in the hydrological and carbon cycles of Amazonian forests and pastures. *Nature* 372, 666–669.
- Nepstad, D.C., Moutinho, P., Dias-Filho, M.B., Davidson, E., Cardinot, G., Markewitz, D., Figueiredo, R., Vianna, N., Chambers, J., Ray, D., Guerreiros, J.B., Lefebvre, P., Sternberg, L., Moreira, M., Barros, L., Ishida, Y., Tohler, I., Belk, E., Kalif, K., Schwalbe, K., 2002. The effects of partial throughfall exclusion on canopy processes, aboveground production, and biogeochemistry of an Amazon forest. *J. Geophys. Res.* 107, 1–18.
- Nepstad, D.C., Lefebvre, P., Da Silva, U.L., Tomasella, J., Schlesinger, P., Solorano, L., Moutinho, P., Ray, D., Benito, J.G., 2004. Amazon drought and its implications for flammability and tree growth: a basin wide analysis. *Glob. Change Biol.* 10 (5), 704–717.
- Nepstad, D.C., Tohver, I.M., Ray, D., Moutinho, P., Cardinot, G., 2007. Mortality of large trees and lianas following experimental drought in an Amazon forest. *Ecology* 88 (9), 2259–2269.
- Oliveira, R.S., Dawson, T.E., Burgess, S.S.O., Nepstad, D.C., 2005. Hydraulic redistribution in three Amazonian trees. *Oecologia* 145, 354–363.
- Potter, C., Klooster, S., Reis de Carvalhi, C., Genovese, V.B., Torregrosa, A., Dungan, J., Bobo, M., Coughlan, J., 2001. Modelling seasonal and interannual variability in ecosystem carbon cycling for the Brazilian Amazon region. *J. Geophys. Res.-Atmos.* 106 (D10), 10.423–10.446.
- Reynolds, W.D., Elrick, D.E., 1991. Determination of hydraulic conductivity using a tension infiltrometer. *Soil Sci. Soc. Am. J.* 55, 633–639.
- Ruivo, M.L.P., Cuhna, E.S., 2003. Mineral and organic components in archaeological black earth and yellow latosol in Caxiuana, Amazon, Brazil. In: Tiezzi, E., Brebbia, C.A., Uso, J.L. (Eds.), *Ecosystems and Sustainable Development*. WIT Press, Southampton, UK, pp. 1113–1121.
- Salazar, L.F., Nobre, C.A., Oyama, M.D., 2007. Climate change consequences on the biome distribution in tropical South America. *Geophys. Res. Lett.* 34, L09708.
- Saleska, S.R., Didan, K., Huete, A.R., da Rocha, H.R., 2007. Amazon forests green-up during 2005 drought. *Science* 318 (5850), 612–613.
- Saleska, S.R., Miller, S.D., Matross, D.M., Goulden, M.L., Wofsy, S.C., da Rocha, H.R., de Camargo, P.B., Crill, P., Daube, B.C., de Freitas, H.C., Hutyra, L., Keller, M., Kirchhoff, V., Menton, M., Munger, J.W., Pyle, E.H., Rice, A.H., Silva, H., 2003. Carbon in Amazon forests: unexpected seasonal fluxes and disturbance-induced losses. *Science* 302 (5650), 1554–1557.
- Sombroek, W., 2001. Spatial and temporal patterns of Amazon rainfall – consequences for the planning of agricultural occupation and the protection of primary forests. *Ambio* 30 (7), 388–396.
- Sperry, J.S., Adler, F.R., Campbell, G.S., Comstock, J.P., 1998. Limitation of plant water use by rhizosphere and xylem conductance: results from a model. *Plant Cell Environ.* 21, 347–359.
- Tian, H.Q., Melillo, J.M., Kicklighter, D.W., McGuire, A.D., Helfrich, J.V.K., Moore, B., Vorosmarty, C.J., 1998. Effect of interannual climate variability on carbon storage in Amazonian ecosystems. *Nature* 396 (6712), 664–667.
- Tomasella, J., Hodnett, M.G., 1996. Soil hydraulic properties and van Genuchten parameters for a oxisol under pasture in central Amazonia. In: Gash, J.H.C., Nobre, A.D., Roberts, J.M., Victoria, R.L. (Eds.), *Amazonian Deforestation and Climate*. Wiley, Chichester, UK, pp. 57–77.
- Tomasella, J., Hodnett, M.G., 1997. Estimating unsaturated hydraulic conductivity of Brazilian soils using soil-water retention data. *Soil Sci.* 162 (10), 703–712.
- van Genuchten, M.T., 1980. A closed form equation for predicting hydraulic conductivity of unsaturated porous materials. *Soil Sci. Soc. Am. J.* 44, 892–898.
- Veldkamp, E., O'Brien, J.J., 2000. Calibration of a frequency domain reflectometry sensor for humid tropical soils of volcanic origin. *Soil Sci. Soc. Am. J.* 64, 1549–1553.
- von Randow, C., Manzi, A.O., Kruijt, B., de Oliveira, P.J., Zanchi, F.B., Silva, R.L., Hodnett, M.G., Gash, J.H.C., Elbers, J.A., Waterloo, M.J., Cardoso, F.L., Kabat, P., 2004. Comparative measurements and seasonal variations in energy and carbon exchange over forest and pasture in South West Amazonia. *Theor. Appl. Climatol.* 78 (1–3), 5–26.
- Werth, D., Avissar, R., 2004. The regional evapotranspiration of the Amazon. *J. Hydrometeorol.* 5 (1), 100–109.
- Williams, M., Rastetter, E.B., Fernandes, D.N., Goulden, M.L., Wofsy, S.C., Shaver, G.R., Melillo, J.M., Munger, J.W., Fan, S.M., Nadelhoffer, K.J., 1996. Modelling the soil-plant-atmosphere continuum in a *Quercus-Acer* stand at Harvard forest: the regulation of stomatal conductance by light, nitrogen and soil/plant hydraulic properties. *Plant Cell Environ.* 19 (8), 911–927.
- Williams, M., Rastetter, E.B., Fernandes, D.N., Goulden, M.L., Shaver, G.R., Johnson, L.C., 1997. Predicting gross primary productivity in terrestrial ecosystems. *Ecol. Appl.* 7, 882–894.
- Williams, M., Malhi, Y., Nobre, A.D., Rastetter, E.B., Grace, J., Pereira, M.G.P., 1998. Seasonal variation in net carbon exchange and evapotranspiration in a Brazilian rainforest: a modelling analysis. *Plant Cell Environ.* 21, 953–968.
- Williams, M., Bond, B.J., Ryan, M.G., 2001. Evaluating different soil and plant hydraulic constraints on tree function using a model and sap flow data from ponderosa pine. *Plant Cell Environ.* 24, 679–690.